



CO₂(ν₂)-O quenching rate coefficient derived from coincidental SABER/TIMED and Fort Collins lidar observations of the mesosphere and lower thermosphere

A. G. Feofilov¹, A. A. Kutepov^{2,3}, C.-Y. She⁴, A. K. Smith⁵, W. D. Pesnell³, and R. A. Goldberg³

¹Centre National de la Recherche Scientifique/École Polytechnique, CNRS/INSU, UMR8539, Palaiseau-Cedex, 91128, France

²The Catholic University of America, Washington DC, 20064, USA

³NASA Goddard Space Flight Center, Greenbelt, MD, 20771, USA

⁴Colorado State University, Fort Collins, CO, 80523, USA

⁵National Center for Atmospheric Research, Boulder, 80307, CO, USA

Correspondence to: A. G. Feofilov (artem.feofilov@lmd.polytechnique.fr)

Received: 24 October 2011 – Published in Atmos. Chem. Phys. Discuss.: 9 December 2011

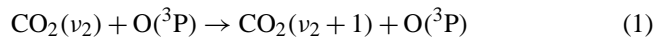
Revised: 31 July 2012 – Accepted: 19 September 2012 – Published: 2 October 2012

Abstract. Among the processes governing the energy balance in the mesosphere and lower thermosphere (MLT), the quenching of CO₂(ν₂) vibrational levels by collisions with O atoms plays an important role. However, there is a factor of 3–4 discrepancy between the laboratory measurements of the CO₂-O quenching rate coefficient, k_{VT} , and its value estimated from the atmospheric observations. In this study, we retrieve k_{VT} in the altitude region 85–105 km from the coincident SABER/TIMED and Fort Collins sodium lidar observations by minimizing the difference between measured and simulated broadband limb 15 μm radiation. The averaged k_{VT} value obtained in this work is $6.5 \pm 1.5 \times 10^{-12} \text{ cm}^3 \text{ s}^{-1}$ that is close to other estimates of this coefficient from the atmospheric observations. However, the retrieved k_{VT} also shows altitude dependence and varies from $5.5 \pm 1.1 \times 10^{-12} \text{ cm}^3 \text{ s}^{-1}$ at 90 km to $7.9 \pm 1.2 \times 10^{-12} \text{ cm}^3 \text{ s}^{-1}$ at 105 km. Obtained results demonstrate the deficiency in current non-LTE modeling of the atmospheric 15 μm radiation, based on the application of the CO₂-O quenching and excitation rates, which are linked by the detailed balance relation. We discuss the possible model improvements, among them accounting for the interaction of the “non-thermal” oxygen atoms with CO₂ molecules.

1 Introduction

Infrared emission in 15 μm CO₂ band ($I_{15 \mu\text{m}}$) is the dominant cooling mechanism in the Earth’s mesosphere and lower thermosphere (MLT, see also Appendix A for the abbreviations not explained in the text for readability’s sake) (Gordiets, 1976; Dickinson, 1984; Goody and Yung, 1989; Sharma and Wintersteiner, 1990). On Earth, the magnitude of the MLT cooling affects both the mesopause temperature and height; the stronger the cooling, the colder and higher is the mesopause (Bougher et al., 1994). This process is also important for the energy budgets of Martian and, especially, Venusian atmospheres (Bougher et al., 1999), where CO₂ cooling compensates for the EUV heating of the dayside upper atmosphere. The $I_{15 \mu\text{m}}$ radiation is used to retrieve vertical temperature distributions $T(z)$ in Earth’s atmosphere by a number of satellite instruments: the CRISTA (Offermann et al., 1999), the SABER (Russell et al., 1999), the MIPAS (Fischer et al., 2008) and in the Martian atmosphere the MGS TES observations (Smith et al., 2001; Feofilov et al., 2012). It is generally accepted that the main mechanism linking the 15 μm CO₂ atmospheric radiation to the heat reservoir (translational degrees of freedom of atmospheric constituents) is the inelastic collision of CO₂ molecules with O(³P) atom; first, atomic O excites the CO₂ bending vibrational mode

during the collision:



after which the excitation may be quenched either by another collision with some molecule or atom or by emission of the radiation quantum: $\text{CO}_2(\nu_2 + 1) \rightarrow \text{CO}_2(\nu_2) + h\nu(667 \text{ cm}^{-1})$, where ν_2 is the bending mode quantum number. Both the cooling efficiency and $I_{15 \mu\text{m}}$ strongly depend on the rate coefficient of the process (1) and on the atomic O volume mixing ratio (VMR). To be consistent with a generally accepted way of describing this process, we will refer to the rate coefficient of the reaction inverse to Eq. (1) and will call it the “CO₂-O quenching rate coefficient” or k_{VT} , where VT index stands for vibrational-translational type of interaction. Generally, it is assumed that the velocity distribution of atomic oxygen is Maxwellian and that the fine structure of atomic oxygen does not affect the process (1) and its inverse. First, we will use these assumptions that are typical for atmospheric modeling and then will address their applicability in the discussion part of the work (Sect. 4).

It is self-evident that both the calculation of radiative cooling/heating rates in CO₂ and the interpretation of measured $I_{15 \mu\text{m}}$ radiation require the best possible knowledge of the k_{VT} (see e.g., Garcia-Comas et al., 2008). However, despite the importance of k_{VT} for the atmospheric applications, the values, obtained in the laboratory and retrieved by fitting the space observations, vary by a factor of 3–4 (see Table 1 and Sect. 2 below for more details). In this work, we describe the retrieving of the k_{VT} from the coincidental space and lidar observations. For this purpose, we used an extensive data set provided by the SABER instrument aboard the TIMED satellite which contains, besides other information, vertical profiles of $I_{15 \mu\text{m}}(z)$ limb radiation, $\text{O}(z)$, and, more recently, $\text{CO}_2(z)$ (Rezac, 2011) VMRs. This dataset was supplemented with $T(z)$ in 80–110 km altitude range measured by the Fort Collins lidar (40.6° N, 105.2° W). We show that the synergy of these two instruments enables one to retrieve k_{VT} and study its behavior in the MLT. The comparison of the SABER temperature retrievals with the Fort Collins lidar measurements has already been done by Remsberg et al. (2008) who found that these data sets agree considering 50 % error in quenching rate ($k_{\text{VT}} = (6.0 \pm 3.0) \times 10^{-12} [\text{cm}^3 \text{ s}^{-1}]$). In this work, we try to make a step forward and get into more details of the MLT physics by applying stringent overlapping criteria and by treating the individual altitude layers of the overlapping region separately. The difference of the present study from the work of Remsberg et al. (2008) is in the k_{VT} retrieval algorithm: instead of comparing the temperatures retrieved with different k_{VT} values, we perform the $k_{\text{VT}}(z)$ estimate by minimizing the differences between the measured and calculated $I_{15 \mu\text{m}}(z)$. All the calculations presented in this work were carried out using the non-LTE ALI-ARMS code package (Kutepov et al., 1998; Gusev and Kutepov, 2003; Feofilov and Kutepov, 2012). The background for the non-LTE problem for the molecular gas

and the review of k_{VT} measurements and estimates is given in the next section.

2 Non-LTE problem for the molecular gas in the atmosphere and k_{VT} rate coefficient

Inelastic molecular collisions determine the population of molecular levels in the lower atmosphere. As a result, local thermodynamic equilibrium (LTE) exists where the populations obey the Boltzmann law with the local kinetic temperature. In the MLT, the frequency of collisions is lower, and the vibrational level populations must be found taking into account all the processes, which populate and depopulate vibrational levels: the absorption of atmospheric and solar radiation in the ro-vibrational bands, spontaneous and stimulated emission, chemical sources, vibrational-vibrational (V-V) and vibrational-translational (V-T) energy exchange processes. The altitude, above which the LTE approximation is not applicable, depends on the relationship between these processes: in general, if the V-T processes dominate or the radiative processes are balanced (optically thick media), the vibrational levels populations are close to LTE. For the CO₂(ν_2) vibrational levels involved in formation of $I_{15 \mu\text{m}}$, the non-LTE effects become significant above ~ 75 – 80 km altitude (López-Puertas and Taylor, 2001; Kutepov et al., 2006; Feofilov and Kutepov, 2012).

The importance of k_{VT} rate coefficient for the calculation of CO₂ emission in the MLT was first discussed by Crutzen (1970). He suggested an estimate for this value with the upper limit of $3.0 \times 10^{-13} \text{ cm}^3 \text{ s}^{-1}$. The first laboratory measurement of k_{VT} was performed at high temperatures ($T > 2000 \text{ K}$) (Center, 1973) using shock tube technique. The extrapolations of these measurements to room temperatures by fitting the Landau-Teller expression (Taylor, 1974) provided the values of about $2.4 \times 10^{-14} \text{ cm}^3 \text{ s}^{-1}$. The average value of this rate coefficient obtained in later studies has changed by two orders of magnitude, and since the middle of 1980-s, the k_{VT} is accepted to be on the order of $(1.0$ – $10.0) \times 10^{-12} \text{ cm}^3 \text{ s}^{-1}$ (see Table 1). However, as we show below, these variations are still large both for the adequate estimation of the radiative budget of the MLT region and for temperature retrievals from $15 \mu\text{m}$ CO₂ radiation. There is a well-known discrepancy between the laboratory measurements of k_{VT} and its retrieval from the atmospheric measurements. Generally, laboratory measurements provide low values of k_{VT} centered around $1.3 \times 10^{-12} \text{ cm}^3 \text{ s}^{-1}$. Huestis et al. (2008), based on the analysis of experimental data and quantum-mechanical calculations, recommend using $k_{\text{VT}} = 1.5 \times 10^{-12} \text{ cm}^3 \text{ s}^{-1}$. However, applying this value to the interpretation of $I_{15 \mu\text{m}}$ measurements leads to overestimating the MLT temperatures. Instead, the values required for an adequate interpreting of atmospheric measurements performed in recent ~ 20 yr are usually about $5.5 \times 10^{-12} \text{ cm}^3 \text{ s}^{-1}$ with the exception of $k_{\text{VT}} = 1.5 \times 10^{-12} \text{ cm}^3 \text{ s}^{-1}$ retrieved by

Vollmann and Grossmann (1997) from the sounding rocket observations.

To demonstrate the influence of k_{VT} on the MLT area, we performed a sensitivity study for an average midlatitude summer atmospheric scenario from MSIS-E-90 model (Hedin, 1991) using a standard set of V-V and V-T rate coefficients (Shved et al., 1998; Kutepov et al., 2006) and the k_{VT} , which was first set to $1.5 \times 10^{-12} \text{ cm}^3 \text{ s}^{-1}$ and then to $6.0 \times 10^{-12} \text{ cm}^3 \text{ s}^{-1}$. The results are presented in Fig. 1a–c. Figure 1a demonstrates the population of the first ν₂-excited level shown as vibrational temperature (see the figure caption for the vibrational temperature definition). Figure 1b shows the sensitivity of the total cooling/heating rate to the k_{VT} change. After obtaining the non-LTE populations of all vibrational levels involved in the task, the broadband $I_{15 \mu\text{m}}$ was simulated in line by line mode and the resulting spectrum was convolved with the “narrow” 15 μm SABER bandpass function for two test runs. The corresponding change in the limb radiance is shown in Fig. 1c. As one can see, the MLT area is sensitive to the k_{VT} changes above ~85 km altitude, which is used as the lower limit for the k_{VT} retrieval in this work. Below this level, the sensitivity rapidly decreases, and 85 km altitude can be considered as a lower limit for the k_{VT} estimates from $I_{15 \mu\text{m}}$ observations. The upper limit of 105 km for the k_{VT} retrieval is defined by the fading of the signal strength with increasing altitude and by the uncertainties in the $O(z)$ distributions.

3 Retrieving k_{VT} from the overlapping SABER and lidar measurements

3.1 The k_{VT} retrieval approach

The general idea for the k_{VT} rate coefficient retrieval from overlapping satellite and lidar measurements is in minimizing the difference between the measured and simulated $I_{15 \mu\text{m}}$ by varying the k_{VT} . The simulations are performed with the “reference” temperature profiles measured by the lidar instrument, which are not affected by the uncertainties in the k_{VT} coefficient. A similar approach was utilized by Feofilov et al. (2009) who used the H₂O VMR profiles measured by the ACE-FTS instrument (Bernath et al., 2005) as reference ones and estimated three rate coefficients necessary for the calculation of H₂O(ν₂) populations in the MLT. Retrieving the k_{VT} from comparing the measured and simulated $I_{15 \mu\text{m}}$ is somewhat more complicated because the CO₂(ν₂) populations depend not only on k_{VT} but also on atomic oxygen concentration (or VMR), which contributes to uncertainties in retrieved k_{VT} . The way of overcoming this limitation will be described below. First, let us consider a simplified case of a single overlap for which everything excluding k_{VT} is known. Since calculations demonstrate monotonic dependence of CO₂(ν₂) populations and limb radiation on k_{VT} at all altitudes (see Fig. 1a, c in this work and

Sect. 3.6.5.1 in López-Puertas and Taylor, 2001), the deviation $\zeta(k_{VT}, z) = |I_{\text{meas}}(z) - I_{\text{simul}}(k_{VT}, z)|$ will have a single minimum at each altitude z and in the ideal case of noiseless signal the retrieved rate coefficient will be unique. Adding noise to the experimental radiation $I_{\text{meas}}(z)$ and adding uncertainties to calculated radiation $I_{\text{simul}}(k_{VT}, z)$, which are linked with uncertainties in lidar temperatures and spatiotemporal variability of the area, respectively, will blur the minimum of $\zeta(k_{VT}, z)$ that will, finally, define the uncertainty for the k_{VT} retrieval. Let us now consider the case, for which both atomic oxygen and k_{VT} are not known. This exercise is necessary since even though the SABER retrieves individual $O(z)$ profiles (Smith et al., 2010), any offsets or errors in $O(z)$ will propagate to k_{VT} . However, this problem might be overcome if the average $O_{\text{aver}}(z)$ profile is known with a sufficient accuracy (from climatology, modeling or other measurements). In this case, one can search for a minimum of $\zeta(\gamma, z)$ with respect to a new variable $\gamma = k_{VT} \times O$ over a large number of the SABER/lidar overlaps. At this stage, individual distributions $O(z)$ are not needed. It is crucial to choose a grid for γ in such a way that the following criteria are satisfied: (a) γ variation range includes the γ_{min} value that corresponds to an absolute minimum of $\zeta(z, \gamma)$; (b) the grid step is fine enough to hit the minimum of $\zeta(z, \gamma)$. When the minimum of $\zeta(z, \gamma)$ is found over a large number of overlaps, one can retrieve the optimal value of rate coefficient: $k_{VT} = \gamma_{\text{min}}/O_{\text{aver}}$ for each altitude point where O_{aver} is the average value of atomic oxygen VMR obtained either from the SABER or the other sources. At this point, the accuracy of $O_{\text{aver}}(z)$ becomes important and will be discussed below. From the methodological point of view, if the dependence of radiance on γ is strongly non-linear, and the γ variability at each altitude is high, then the retrieval approach should be modified and the corresponding $\zeta(k_{VT}, z)$ should include the weights, which are proportional to the radiance responses at given γ . However, as the analysis performed for this work shows, non-linear effects have little influence on the retrieved k_{VT} for the conditions considered in this work.

3.2 Using the Colorado State Sodium lidar temperature measurements for k_{VT} retrievals

In this study, we used $I_{15 \mu\text{m}}(z)$, $T(z)$, $P(z)$, CO₂(z), and $O(z)$ from the SABER V1.07 database and coincidental $T(z)$ measured by the Colorado State Sodium lidar described in details in (She et al., 2003). Briefly, the lidar is a two-beam system capable of simultaneous measurement of the mesopause region temperature and winds, day and night, weather permitting. This lidar was modified in 1999 in response to TIMED satellite objectives. The lidar setup can perform simultaneous measuring of the mesopause region Na density, temperature, zonal and meridional wind profiles with both daytime and nighttime capability. The measurement precision of the lidar system for temperature and wind with 2 km spatial resolution and 1 h integration time

Table 1. Historical review of the $k_{VT}\{\text{CO}_2\text{-O}\}$ quenching rate coefficient measurements and atmospheric retrievals at $T = 300\text{ K}$.

$k_{VT}\{\text{CO}_2\text{-O}\} [\text{cm}^3\text{s}^{-1}]$	Reference	Comments
$3\text{--}30 \times 10^{-14}$	Crutzen (1970)	First guess
2.4×10^{-14}	Taylor (1974), Center (1973)	Laboratory measurements
5.0×10^{-13}	Sharma and Nadille (1981)	Atmospheric retrieval
1.0×10^{-12}	Gordiets et al. (1982)	Numerical experiment
2.0×10^{-13}	Kumer and James (1983)	Atmospheric retrieval
2.0×10^{-13}	Dickinson (1984); Allen (1980)	Laboratory measurements
5.2×10^{-12}	Stair et al. (1985)	Atmospheric retrieval
3.5×10^{-12}	Sharma (1987)	Atmospheric retrieval
$3\text{--}9 \times 10^{-12}$	Sharma and Wintersteiner (1990)	Atmospheric retrieval
1.5×10^{-12}	Shved et al. (1991)	Laboratory measurements
$3\text{--}6 \times 10^{-12}$	López-Puertas et al. (1992)	Atmospheric retrieval
1.3×10^{-12}	Pollock et al. (1993)	Laboratory measurements
5.0×10^{-12}	Ratkowski et al. (1994)	Atmospheric retrieval
5.0×10^{-13}	Lilenfeld (1994)	Laboratory measurements
1.5×10^{-12}	Vollmann and Grossmann (1997)	Atmospheric retrieval
1.4×10^{-12}	Khvorostovskaya et al. (2002)	Laboratory measurements
1.8×10^{-12}	Castle et al. (2006)	Laboratory measurements
6.0×10^{-12}	Gusev et al. (2006)	Atmospheric retrieval
1.5×10^{-12}	Huestis et al. (2008)	Recommended value
$1.3\text{--}2.7 \times 10^{-12}$	Castle et al. (2012)	Laboratory measurements

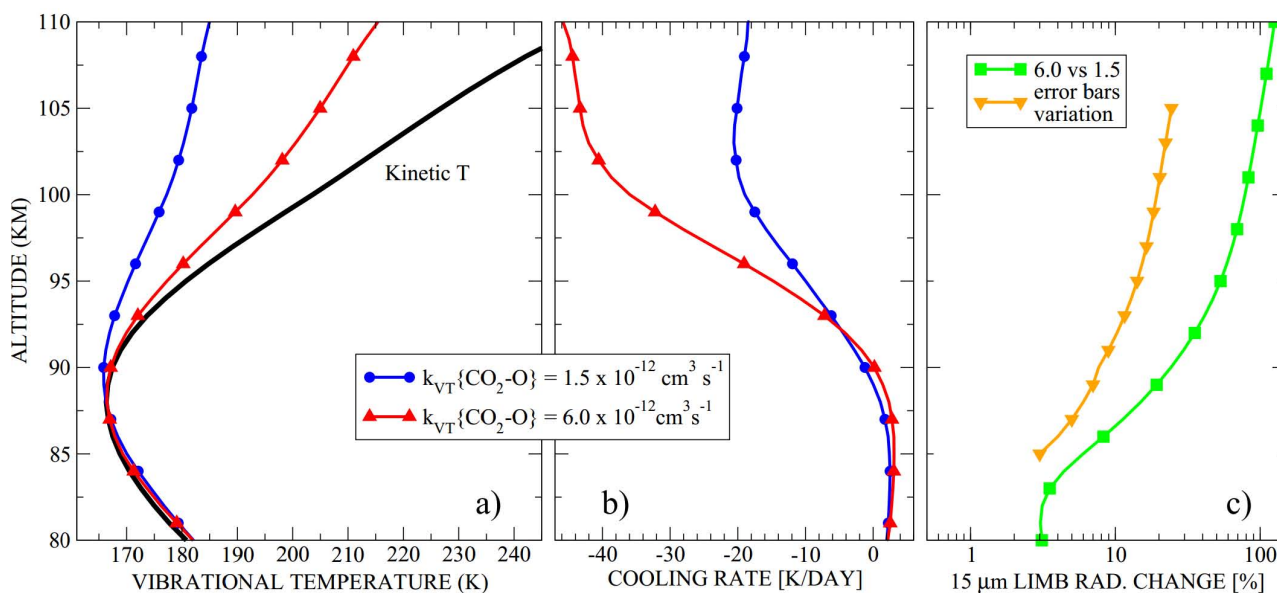


Fig. 1. The sensitivity of (a) CO₂(010) main isotope vibrational level populations, (b) infrared cooling/heating rate in CO₂ bands, and (c) $I_{15\text{ }\mu\text{m}}(z)$ to k_{VT} . For panels (a) and (b): lines with circles correspond to $k_{VT} = 1.5 \times 10^{-12} \text{ cm}^3 \text{ s}^{-1}$ and lines with triangles correspond to $k_{VT} = 6.0 \times 10^{-12} \text{ cm}^3 \text{ s}^{-1}$. The non-LTE populations in panel (a) are presented as vibrational temperatures, which represent the vibrational level excitation against the ground level 0: $n_1/n_0 = g_1/g_0 \exp[-(E_1 - E_0)/kT_v]$, where $n_{0,1}$, $g_{0,1}$, and $E_{0,1}$ are populations, degenerations, and energies of the ground state and first vibrational level, respectively. The atmospheric model used for this sensitivity study is the midlatitude summer profile of temperature, pressure, and atomic oxygen VMR from the MSIS-E-90 combined with the WACCM CO₂ VMR profile for the corresponding conditions. The curves with squares/triangles in panel (c) show the $I_{15\text{ }\mu\text{m}}(z)$ responses for the cases when the k_{VT} changes from 1.5 to $6.0 \times 10^{-12} \text{ cm}^3 \text{ s}^{-1}$ and varies within estimated uncertainties in Fig. 2c, correspondingly (see also the discussion in Sect. 4).

were estimated for each beam under nighttime fair sky conditions to be, respectively, 0.5 K and 1.5 m s⁻¹ at the Na peak (92 km), and 5 K and 15 m s⁻¹ at the edges (81 and 107 km) of the Na layer. Depending on the purpose of the analysis, the temporal resolution may be made between 10 min and several hours. We have searched for the SABER/lidar simultaneous common volume measurements in 2002–2005 using stringent criteria for time and space overlapping: $\Delta \text{lat} < 2^\circ$, $\Delta \text{long} < 2^\circ$, $\Delta t < 10 \text{ min}$. Most of the profiles selected in way (85 %) fall in 18–6 h local time interval. We substituted the SABER $T(z)$ in 80–110 km altitude range with the corresponding lidar $T(z)$ and hydrostatically adjusted $P(z)$ to new $T(z)$. Atomic O is changing in this period and using individual $O(z)$ is not reasonable; therefore, we used the $\gamma = k_{VT} \times O$ variable discussed in Sect. 3.1. To reduce the number of runs with obviously incorrect γ values, we used the following approach: at each altitude the grid on γ was built using the available $O(z)$ and 21 points for k_{VT} in the $(1.0\text{--}10) \times 10^{-12} \text{ cm}^3 \text{ s}^{-1}$ range with $5 \times 10^{-13} \text{ cm}^3 \text{ s}^{-1}$ step. The correctness of the γ grid selection was verified at each altitude and for each overlapping event by checking for the existence of the $\zeta(\gamma, z)$ minimum. For each overlapping event, the non-LTE populations of CO₂ vibrational levels were found at all altitudes and $I_{15 \mu\text{m}}$ was simulated in line by line mode and then convolved with the corresponding SABER bandpass function. This procedure was repeated for all grid points of the γ variable. Then at each altitude point z we calculated the radiation difference $\zeta(\gamma, z)$ (Fig. 2a). All $\zeta(\gamma, z)$ curves up to 105 km (cyan curve) have a clear minimum $\zeta_{\text{min}}(\gamma, z)$ that washes out for $\zeta(\gamma, z)$ dependencies above that altitude (not shown in Fig. 2a). This behavior is explained both by larger lidar $T(z)$ and by larger $I_{15 \mu\text{m}}(z)$ uncertainties at higher altitudes. The values of γ corresponding to $\zeta_{\text{min}}(\gamma, z)$ form a separate scientific product $\gamma_{\text{min}}(z)$ that may be used in midlatitude atmospheric applications for the $I_{15 \mu\text{m}}$ calculations. The retrieved $\gamma_{\text{min}}(z)$ values are 1.1×10^{-14} ; 5.7×10^{-14} ; 2.0×10^{-13} ; 5.1×10^{-13} ; $6.4 \times 10^{-13} [\text{cm}^3 \text{ s}^{-1}]$ for $z = 85$; 90; 95; 100; 105 km, respectively. To obtain the $k_{VT}(z)$ profile (Fig. 2c) we divided the $\gamma_{\text{min}}(z)$ profile by average atomic O VMR profile, $O_{\text{aver}}(z)$, (Fig. 2b). The dashed lines in Fig. 2c represent standard deviations estimated from input data uncertainties.

4 Discussion

Overall, the $k_{VT}(z)$ values shown in Fig. 2c fit well to the atmospheric retrievals: the averaged value of k_{VT} is equal to $6.5 \pm 1.5 \times 10^{-12} \text{ cm}^3 \text{ s}^{-1}$. However, Fig. 2c also demonstrates the altitudinal variability of $k_{VT}(z)$ that goes slightly beyond its uncertainties in 85–105 km altitude range. Obviously, this variability does not imply that k_{VT} rate coefficient depends on altitude. Let us consider possible reasons for the observed k_{VT} behavior. The retrieved $k_{VT}(z)$ depends on: (a) lidar $T(z)$ in 80–110 km, (b) the SABER $P(z)$ and $T(z)$

below 80 km, (c) $I_{15 \mu\text{m}}(z)$ (d) CO₂(z), (e) O(z), (f) CO₂ non-LTE model. Offsets in any of these parameters will lead to offsets in the retrieved $k_{VT}(z)$. The quality of the SABER V1.07 product has been evaluated by Remsberg et al. (2008). As they show, in general, SABER V1.07 temperatures are 1–3 K higher than lidar in the lower stratosphere and $\sim 1\text{--}3$ K lower than lidar in the upper stratosphere and lower mesosphere. Assuming a 3 K positive temperature change in the lower stratosphere and 3 K negative temperature change in the upper stratosphere and lower mesosphere, we have estimated $I_{15 \mu\text{m}}$ limb radiation change above 85 km. In this test performed for the mid-latitude atmospheric scenario, the pressure profile has been hydrostatically adjusted, the non-LTE populations have been found, and $I_{15 \mu\text{m}}$ has been calculated and compared to $I_{15 \mu\text{m}}$ calculated for unperturbed pressure/temperature distribution. This test shows that changes in $I_{15 \mu\text{m}}$ above 85 km do not exceed 1 %. At the same time, the sensitivity of $I_{15 \mu\text{m}}$ to k_{VT} change within the error bars is much higher: 4 % at 85 km, 8 % at 90 km, 15 % at 95 km, 20 % at 100 km, and 25 % at 105 km (see a solid curve with triangles in Fig. 1c). Correspondingly, the propagation of the systematic error in pressure/temperature distributions below 85 km to the area of our particular interest through hydrostatics is negligible. The main contributor to the 15 μm upwelling radiative flux at the mesospheric altitudes is the stratopause area where temperatures are high and the concentration of the emitters is still high. In this area, SABER temperatures are in reasonable agreement with other measurements (Remsberg et al., 2008), and the uncertainty of the upwelling flux associated with temperature uncertainty can be estimated as ± 2 %. There are not too many CO₂(z) data sets for the MLT area. In Fig. 3a we show the average vertical distributions of CO₂, which were calculated in WACCM model (Garcia et al., 2007; Smith et al., 2011), retrieved from SABER V1.07 in (Rezac, 2011), and retrieved from the ACE-FTS occultation observations (Beagley et al., 2010). The distributions agree within standard deviation limits (shown only for ACE-FTS for readability of the plot, the others are of the same order of magnitude). We did not consider CRISTA CO₂ distributions (Kaufmann et al., 2002) because there was no temporal overlap with the data sets used in the present study: almost 10 yr have passed since the CRISTA-2 operation.

The most critical component for the $k_{VT}(z)$ retrieval is $O_{\text{aver}}(z)$. A detailed analysis of the SABER V1.07 data shows that the O density is at least twice that from several other data sources (Smith et al., 2010 and references therein). However, reducing $O_{\text{aver}}(z)$ by factor of two will mean increasing $k_{VT}(z)$ by the same factor, which will make it 8–10 times larger than the laboratory measured values (line with squares in Fig. 3b). On the other hand, there is increasing evidence for the reliability of the O determined from SABER (Xu et al., 2012) and additional observations with similar high O VMRs (Sheese et al., 2011). The retrieval of O(z) in the SABER V1.07 also depends on temperature. However, as discussed by Smith et al. (2010), the contributions

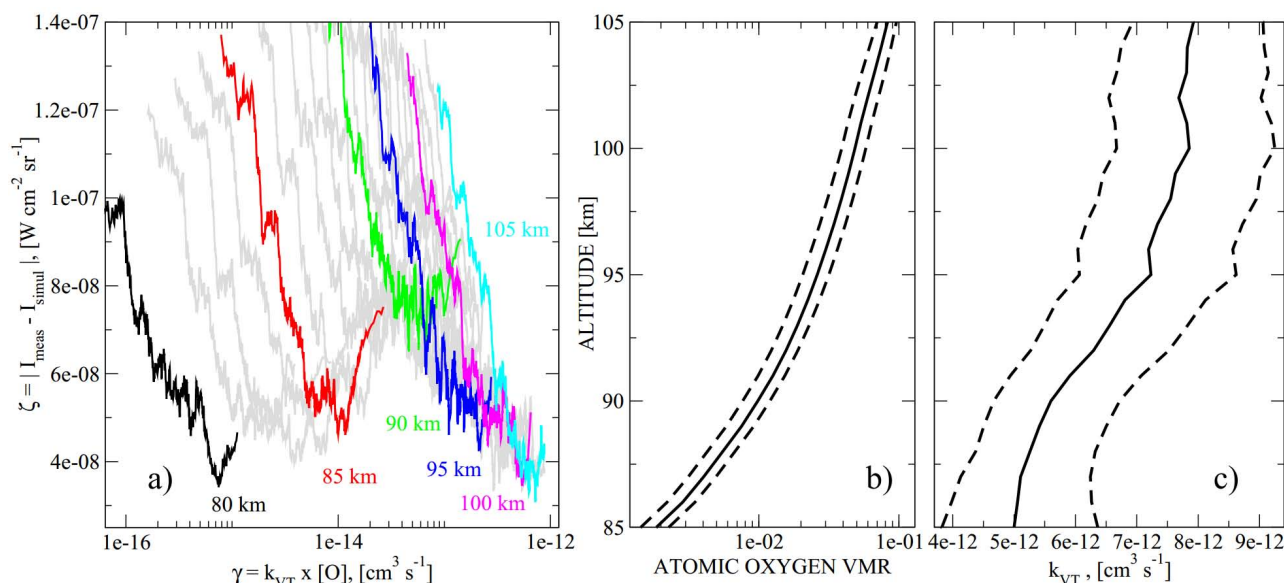


Fig. 2. Estimating the optimal k_{VT} from the overlapping SABER and lidar measurements: (a) deviations between calculated and measured $I_{15\mu\text{m}}$ at different altitudes with respect to a combined γ value (see text). Each $\zeta(\gamma, z)$ curve in this panel represents the average over 72 individual deviations. Note the existence of $\zeta(\gamma, z)$ minima at all heights up to 105 km (cyan curve); (b) solid line: average $O(z)$ built for all overlapping events, dashed lines: standard deviations for $O(z)$ estimated in Mlynčzak et al. (2012); (c) solid line: $k_{VT}(z)$ obtained as a result of dividing the individual minima found in the left panel by atomic O VMRs from the middle panel; dashed lines: standard deviations for k_{VT} .

of uncertainties in temperature to $O(z)$ are small. Moreover, any appreciable errors in temperatures would upset the excellent agreement between daytime and nighttime $O(z)$ (see discussion in Smith et al., 2010). In this work, we have used the $O(z)$ uncertainties from (Mlynčzak et al., 2012) for the $k_{VT}(z)$ error bars estimates shown in Fig. 2c.

It is worth noting that the altitude dependence of the retrieved $k_{VT}(z)$ follows the temperature distribution in the MLT. As the quantum-mechanical calculations show (de Lara-Castells et al., 2006), the vibrational quenching of CO₂(v₂) is significantly enhanced by spin-orbit interaction, the probability of which depends on energy, so positive temperature dependency should be expected. In the present study we already used a standard $(T/300)^{1/2}$ temperature scaling of k_{VT} , so one has to assume that the temperature dependency is stronger than $T^{1/2}$. However, the most recent laboratory measurements of k_{VT} in the 142–490 K temperature range (Castle et al., 2012) do not confirm this prediction and demonstrate negative temperature dependency. In Fig. 3b we show $k_{VT}(z)$ estimates for this case. As one can see, k_{VT} almost reaches the value of $1.2 \times 10^{-11} \text{ cm}^3 \text{ s}^{-1}$ at 105 km. We believe that the contradiction between laboratory measurements and theoretical estimates of temperature dependency of k_{VT} is just another hint for deficiency of the CO₂ non-LTE model with respect to CO₂-O collisions, which will be discussed further.

The standard pumping term in the non-LTE model, which describes total production of CO₂(v₂) in the state with the

number of bending mode quanta v_2 due to collisions with the O(³P) atoms has the form of

$$Y_{v_2} = n_{O(^3P)} \{n_{v_2-1} k_{v_2-1, v_2} - n_{v_2} k_{v_2, v_2-1}\} \quad (2)$$

where $n_{O(^3P)}$ is the O(³P) density, n_{v_2-1} and n_{v_2} are the vibrational states populations, and k_{v_2-1, v_2} and k_{v_2, v_2-1} are rate coefficients for one-quantum excitation and de-excitation, respectively. In current non-LTE models, including the one applied in this study, it is usually assumed that $k_{v_2-1, v_2} = k_{0,1}$ and $k_{v_2, v_2-1} = k_{1,0}$. It follows from Huestis et al. (2008) that if the velocity distribution of O(³P) atoms is Maxwellian and their fine structure is thermalized then the laboratory measured $k_{0,1}$ and $k_{1,0}$ are linked by the detailed balance relation:

$$k_{0,1} = k_{1,0} \cdot \frac{g_1}{g_0} \cdot e^{-E_1/kT} \quad (3)$$

where g_0 and g_1 are the statistical weights of the lower and upper vibrational states, respectively, E_1 is the vibrational energy of the first v_2 vibrational level, k is the Boltzmann constant, and T is the local kinetic temperature. Sharma et al. (1994) showed that both above-mentioned conditions are valid for O(³P) atoms in the Earth's atmosphere up to at least 400 km, which seems to justify usage of Eqs. (2) and (3) in the non-LTE models. However, as Balakrishnan et al. (1998) and Kharchenko et al. (2005) show, the non-thermal O(³P) and O(¹D) atoms are produced by O₂ and O₃ photolysis and

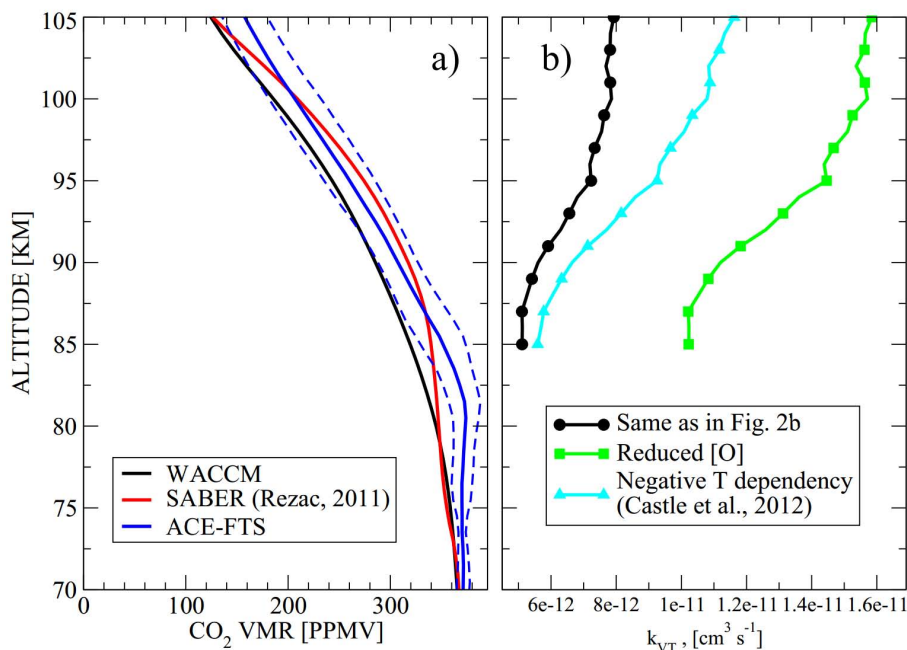


Fig. 3. (a) Average vertical distributions of CO₂ VMR distributions for 40.6 ± 2° N in 2002–2009 for WACCM and SABER, and in 2008–2009 for ACE-FTS. Dashed blue lines denote standard deviation for the ACE-FTS CO₂ profile; (b) estimated vertical profile of $k_{VT}(z)$ for O(z) divided by 2 and for a negative temperature dependency of k_{VT} according to the latest laboratory measurements (Castle et al., 2012).

O₂⁺ dissociative recombination reactions in the MLT. These “hot” atoms may serve as an additional source of CO₂(ν₂) level excitation. Therefore, the expression (2) may need to be replaced by an expression like

$$Y_{\nu_2} = n_{O(^3P)} \cdot \left[(1 - \alpha) \cdot \{ n_{\nu_2-1} k_{\nu_2-1, \nu_2} - n_{\nu_2} k_{\nu_2, \nu_2-1} \} + \alpha \cdot \left\{ \sum_{\nu} n_{\nu_2-\nu} k_{\nu_2-\nu, \nu_2}^{\text{hot}} - n_{\nu_2} \sum_{\nu} k_{\nu_2, \nu_2-\nu}^{\text{hot}} \right\} \right] \quad (4)$$

where α is the fraction of total O(³P) density, which corresponds to hot atoms, $k_{\nu_2-\nu, \nu_2}^{\text{hot}}$ and $k_{\nu_2, \nu_2-\nu}^{\text{hot}}$ are the rate coefficients for excitation and de-excitation of CO₂ molecules, respectively, due to collisions with hot atoms, assuming also multi-quantum processes. These rate coefficients are not related by the detailed balance since hot O(³P) atoms are not thermalized. Comparing Eq. (2) which is applied in the model used in our study with Eq. (4), one can see that the rate coefficient values retrieved in this work and in other atmospheric studies are some sort of effective rate coefficient. This may be expressed as

$$k_{1,0}^{\text{retr}}(z) = k_{\nu_2, \nu_2-1}^{\text{retr}}(z) = (1 - \alpha(z)) \cdot k_{\nu_2-1, \nu_2} + \alpha(z) \cdot \sum_{\nu} n_{\nu_2} k_{\nu_2-\nu, \nu_2}^{\text{hot}} \quad (5)$$

which includes the contribution of hot O(³P) atoms. We note here that the $k_{\nu_2-\nu, \nu_2}^{\text{hot}}$ in Eq. (5) relates only to the pumping term and, therefore, $k_{1,0}^{\text{retr}}$, strictly speaking, should not be treated as a reaction coefficient of the balanced process

anymore, which is important for the future studies of this problem. In addition to non-thermal oxygen, one can also consider other sources of collisional excitation as, for example, collisions with thermal and non-thermal hydrogen, electronically-excited atomic oxygen O(¹S), charged components, or multi-quantum excitation of CO₂ by thermal oxygen (Ogibalov, 2000). In any case, the effective collisional rate coefficient and the VMR of this “unknown” component with respect to O(z) may be represented in a way similar to Eq. (5). However, in the case of multi-quantum excitation $k_{\nu_2-\nu, \nu_2}^{\text{hot}}$ must be replaced with the multi-quantum excitation rate, while $\alpha(z)$ in this approach should be constant with altitude, which is in contradiction with variable $k_{VT}(z)$ observed in the present study.

Simple calculations show that assuming k_{ν_2-1, ν_2} to be fixed at $(5.0) \times 10^{-12}$ [cm³ s⁻¹], the rate coefficients for the collisions with hot oxygen, $k_{\nu_2-\nu, \nu_2}^{\text{hot}}$, should be 10 times larger than k_{ν_2-1, ν_2} and $\alpha(z)$ should vary linearly from 0% at 85 km to 2% at 105 km in order to account for the observed $k_{VT}(z)$ increase with altitude. As Kharchenko et al. (2005) show, the hot oxygen fraction at these heights is ~ 5% during daytime. Even though most of the overlapping profiles used in this work fall in 18–6 h local time interval, the MLT area is illuminated by the sun in at least half of the selected events (the shadow level at 100 km corresponds to solar zenith angle $\theta_z = 101^\circ$, and the average θ_z is $105 \pm 30^\circ$). The magnitudes of $k_{\nu_2-\nu, \nu_2}^{\text{hot}}$ are larger than k_{ν_2-1, ν_2} (Shizgal, 1979) though obtaining the exact values requires complicated

quantum-mechanical calculations (V. Kharchenko, personal communication, 2011). It is also important to calculate the thermalization timescales for hot oxygen atoms. To summarize: the concept of hot oxygen as an additional pumping source for the CO₂(ν₂) levels is a *possible* explanation of the $k_{VT}(z)$ variation and the discrepancy between laboratory measurements and atmospheric estimates of this rate coefficient. Of course, the simplified analysis given above is not intended to be the ultimate explanation of our result. However, it may indicate the direction toward its interpretation.

5 Summary

In this work, we discussed a refined methodology for retrieving k_{VT} , the quenching rate for the ν₂ vibrations of CO₂ molecules by collisions with O atoms. The suggested approach differs from those used in the previous studies (see the “atmospheric retrieval” values in Table 1), where the k_{VT} was retrieved by fitting the measurements of the CO₂ 15 μm emissions. The method (a) combines space-borne radiance measurements with the ground-based (i.e. lidar) temperature observations, (b) allows retrieving k_{VT} independently at various altitudes, (c) allows retrieving the parameter $\gamma = k_{VT} \times O$ (where O is the VMR of atomic oxygen), which is the contribution of atomic oxygen quenching to the total quenching rate of the CO₂(ν₂) vibrations. Using the γ variable instead of the k_{VT} in minimizing the difference between measured and simulated limb radiance significantly improves the stability and accuracy of retrieving.

The suggested technique is applied to the overlapping SABER/TIMED (15 μm radiance, CO₂ and O(³P) VMRs) and Fort Collins lidar temperature measurements. The obtained γ values are 1.1×10^{-14} ; 5.7×10^{-14} ; 2.0×10^{-13} ; 5.1×10^{-13} ; 6.4×10^{-13} [cm³ s⁻¹] at 85; 90; 95; 100; 105 km, respectively. The average value of the retrieved k_{VT} in 85–105 km altitude range is $6.5 \pm 1.5 \times 10^{-12}$ cm³ s⁻¹ that is in excellent agreement with other values estimated from space-borne observations. However, we also observed an altitude dependence of the retrieved k_{VT} , which varies from $5.5 \pm 1.1 \times 10^{-12}$ cm³ s⁻¹ at 85 km to $7.9 \pm 1.2 \times 10^{-12}$ cm³ s⁻¹ at 105 km. We link the observed variation as well as the discrepancy between the “atmospheric” and laboratory measurements to a simplification in the traditional consideration of CO₂(ν₂)+O(³P) interactions in the current non-LTE models, including the model applied in this study, where the rate coefficients of the vibrational quenching and excitation are linked by the detailed balance relation. We discuss that both problems may be explained by interaction of CO₂ molecules with the hot oxygen atoms, which is missing in the current models. We subdivide the oxygen atoms in the MLT to “normal” and “excited” or “hot” groups, with different k_{VT} rate coefficients for each of the groups and keep in mind that rate coefficients for the former group are balanced, whereas those for the lat-

ter group do not obey the detailed balance relation. Further studies to explain the current results are needed including (a) quantum-mechanical calculations for the collisions of CO₂ with “hot” O atoms and, possibly, other atmospheric components needed to improve the non-LTE model of the IR emission formation in the MLT, (b) new comparisons of space radiance observations with the lidar temperature measurements at various locations (including those for polar regions). The radiative cooling rate calculations for general circulation models and calculations of the emerging IR radiation will obviously depend on the mechanism of interaction between the radiation field and atmosphere, which will be revealed in the course of these additional studies. However, one result follows already from the present work: for the practical temperature retrievals from the 15 μm CO₂ atmospheric radiation observations, the $k_{1,0}^{ret}(z)$ values obtained in this study may be recommended. As we show in our discussion, at the current stage of the non-LTE model development these values provide better presentation of the CO₂-O interactions, which relies at best fitting of coincidental atmospheric radiance and ground based temperature observations.

Appendix A

Abbreviations

ACE FTS	Fourier-Transform Spectrometer in Atmospheric Chemistry Experiment
ALI-ARMS	Accelerated Lambda Iterations for Atmospheric Radiation and Molecular Spect
ASTRO-SPAS CRISTA	Astronomical Shuttle-Pallet Satellite Cryogenic Infrared Spectrometers and Telescopes for the Atmosphere, on board the ASTRO-SPAS satellite
EUV	Extreme Ultraviolet
LTE	Local Thermodynamic Equilibrium
MGS TES	Thermal Emission Spectrometer onboard Mars Global Surveyor satellite
MIPAS	Michelson Interferometer for Passive Atmospheric Sounding
MLT	Mesosphere/Lower Thermosphere
SABER	Sounding of the Atmosphere using Broadband Emission Radiometry
TIMED	Thermosphere Ionosphere Mesosphere Energetics and Dynamics
VMR	Volume Mixing Ratio
WACCM	Whole Atmosphere Community Climate Model

Acknowledgements. This research was partially supported under NASA grant NNX08AG41G. NCAR is sponsored by the National Science Foundation. The authors would like to thank Peter Wintersteiner and Richard Picard for their comments on the preliminary version of the manuscript, David Huestis for the discussion

regarding the detailed balance in CO₂(ν₂) + O(³P) collisions, Vasili Kharchenko for the discussion regarding non-thermal oxygen atoms, Martin Mlynczak for the discussion regarding SABER O(³P) retrieval and its uncertainties, Ladislav Rezac for the discussion regarding the SABER CO₂ VMR retrievals, and Svetlana Petelina for providing the ACE-FTS CO₂ vertical distributions.

Edited by: W. Ward



The publication of this article is financed by CNRS-INSU.

References

- Allen, D. C., Scragg, T., and Simpson, C. J. S. M.: Low temperature fluorescence studies of the deactivation of the bend-stretch manifold of CO₂, *Chem. Phys.*, 51, 279–298, 1980.
- Balakrishnan, N., Kharchenko, V., and Dalgarno, A.: Slowing of energetic O(³P) atoms in collisions with N₂, *J. Geophys. Res.*, 103, 23393–23398, 1998.
- Beagley, S. R., Boone, C. D., Fomichev, V. I., Jin, J. J., Semeniuk, K., McConnell, J. C., and Bernath, P. F.: First multi-year occultation observations of CO₂ in the MLT by ACE satellite: observations and analysis using the extended CMAM, *Atmos. Chem. Phys.*, 10, 1133–1153, doi:10.5194/acp-10-1133-2010, 2010.
- Bernath, P. F., McElroy, C. T., Abrams, M. C., Boone, C. D., Butler, M., Camy-Peyret, C., Carleer, M., Clerbaux, C., Coheur, P. F., Colin, R., DeCola, P., DeMazière, M., Drummond, J. R., Dufour, D., Evans, W. F. J., Fast, H., Fussen, D., Gilbert, K., Jennings, D. E., Llewellyn, E. J., Lowe, R. P., Mahieu, E., McConnell, J. C., McHugh, M., McLeod, S. D., Michaud, R., Midwinter, C., Nassar, R., Nichitui, F., Nowlan, C., Rinsland, C. P., Rochon, Y. J., Rowlands, N., Semeniuk, K., Simon, P., Skelton, R., Sloan, J. J., Soucy, M.-A., Strong, K., Tremblay, P., Turnbull, D., Walker, K. A., Walkty, I., Wardle, D. A., Wehrle, V., Zander, R., and Zou, J.: Atmospheric Chemistry Experiment (ACE): Mission overview, *Geophys. Res. Lett.*, 32, L15S01, doi:10.1029/2005GL022386, 2005.
- Bougher, S. W., Hunten, D. M., and Roble, R. G.: CO₂ cooling in terrestrial planet thermospheres, *J. Geophys. Res.*, 99, 14609–14622, 1994.
- Bougher, S. W., Engel, S., Roble, R. G., and Foster, B.: Comparative Terrestrial Planet Thermospheres: 2. Solar Cycle Variation of Global Structure and Winds at Equinox, *J. Geophys. Res.*, 104, 16591–16611, 1999.
- Castle, K. J., Kleissas, K. M., Rhinehart, J. M., Hwang, E. S., and Dodd, J. A.: Vibrational relaxation of CO₂(ν₂) by atomic oxygen, *J. Geophys. Res.*, 111, A09303, doi:10.1029/2006JA011736, 2006.
- Castle, K. J., Black, L. A., Simone, M. W., and Dodd, J. A.: Vibrational Relaxation of CO₂(ν₂) by O(³P) in the 142–490 K Temperature Range, *J. Geophys. Res.*, 117, A04310, doi:10.1029/2012JA017519, 2012.
- Center, R. E.: Vibrational relaxation of CO₂ by O atoms, *J. Chem. Phys.*, 59, 3523–3528, 1973.
- Crutzen, P. J.: Discussion of paper “Absorption and emission by carbon dioxide in the atmosphere” by J. T. Houghton, *Quart. J. Roy. Met. Soc.*, 96, 767–770, 1970.
- Dickinson, R. E.: Infrared radiative cooling in the mesosphere and lower thermosphere, *J. Atmos. Sol. Terr. Phys.*, 46, 995–1008, 1984.
- Feofilov, A. G. and Kutepov, A. A.: Infrared radiation in the mesosphere and lower thermosphere: energetic effects and remote sensing, *Surv. Geophys.*, doi:10.1007/s10712-012-9204-0, in press, 2012.
- Feofilov, A. G., Kutepov, A. A., Pesnell, W. D., Goldberg, R. A., Marshall, B. T., Gordley, L. L., García-Comas, M., López-Puertas, M., Manuilova, R. O., Yankovsky, V. A., Petelina, S. V., and Russell III, J. M.: Daytime SABER/TIMED observations of water vapor in the mesosphere: retrieval approach and first results, *Atmos. Chem. Phys.*, 9, 8139–8158, doi:10.5194/acp-9-8139-2009, 2009.
- Feofilov, A. G., Kutepov, A. A., Rezac, L., and Smith, M. D.: Extending MGS-TES Temperature Retrievals in the Martian Atmosphere up to 90 km: Retrieval Approach and Results, *Icarus*, in press, 2012.
- Fischer, H., Birk, M., Blom, C., Carli, B., Carlotti, M., von Clarman, T., Delbouille, L., Dudhia, A., Ehhalt, D., Endemann, M., Flaud, J. M., Gessner, R., Kleinert, A., Koopman, R., Langen, J., López-Puertas, M., Mosner, P., Nett, H., Oelhaf, H., Perron, G., Remedios, J., Ridolfi, M., Stiller, G., and Zander, R.: MIPAS: an instrument for atmospheric and climate research, *Atmos. Chem. Phys.*, 8, 2151–2188, doi:10.5194/acp-8-2151-2008, 2008.
- García, R. R., Marsh, D. R., Kinnison, D. E., Boville, B. A., and Sassi, F.: Simulation of secular trends in the middle atmosphere, 1950–2003, *J. Geophys. Res.*, 112, D09301, doi:10.1029/2006JD007485, 2007.
- García-Comas, M., López-Puertas, M., Marshall, B. T., Wintersteiner, P. P., Funke, B., Bermejo-Pantaleón, D., Mertens, C. J., Remsberg, E. E., Gordley, L. L., Mlynczak, M. G., and Russell III, J. M.: Errors in Sounding of the Atmosphere using Broadband Emission Radiometry (SABER) kinetic temperature caused by non-local-thermodynamic-equilibrium model parameters, *J. Geophys. Res.*, 113, D24106, doi:10.1029/2008JD010105, 2008.
- Goody, R. M. and Yung, Y. L.: *Atmospheric Radiation*, Oxford Univ. Press, New York, NY, 1989.
- Gordiets, B. F.: A model of the upper atmosphere radiating in infrared spectrum, *Kratkie Soobsh. Fiz.*, 6, 40, 1976.
- Gordiets, B. F., Kulikov, Yu. N., Markov, M. N., and Marov, M. Ya.: Numerical Modelling of the Thermospheric Heat Budget, *J. Geophys. Res.*, 87, 4504–4514, 1982.
- Gusev, O. A. and Kutepov, A. A.: Non-LTE gas in planetary atmospheres, in *Stellar Atmosphere Modeling*, ASP Conference Series, 288, edited by: Hubeny, I., Mihalas, D., and Werner, K., 318–330, 2003.
- Gusev, O., Kaufmann, M., Grossmann, K. U., Schmidlin, F. J., and Shepherd, M. G.: Atmospheric neutral temperature distribution at the mesopause/turbopause altitude, *J. Atmos. Sol. Terr. Phys.*, 68, 1684–1697, doi:10.1016/j.jastp.2005.12.010, 2006.

- Hedin, A. E.: Extension of the MSIS thermosphere model into the middle and lower atmosphere, *J. Geophys. Res.*, 96, 1159–1172, 1991.
- Huestis, D. L., Bougher, S. W., Fox, J. L., Galand, M., Johnson, R. E., Moses, J. I., and Pickering, J. C.: Cross Sections and Reaction Rates for Comparative Planetary Aeronomy, *Space Sci. Rev.*, 139, 63–105, doi:10.1007/s11214-008-9383-7, 2008.
- Kaufmann, M., Gusev, O. A., Grossmann, K. U., Roble, R. G., Hagan, M. E., Hartsough, C., and Kutepov, A. A.: The vertical and horizontal distribution of CO₂ densities in the upper mesosphere and lower thermosphere as measured by CRISTA, *J. Geophys. Res.*, 107, 8182–8200, doi:10.1029/2001JD000704, 2002.
- Kharchenko, V., Dalgarno, A., and Fox, J. L.: Thermospheric distribution of fast O(¹D) atoms, *J. Geophys. Res.*, 110, A12305, doi:10.1029/2005JA011232, 2005.
- Khvorostovskaya, L. E., Yu. Potekhin, I., Shved, G. M., Ogibalov, V. P., and Uzyukova, T. V.: Measurement of the Rate Constant for Quenching CO₂(01¹0) by Atomic Oxygen at Low Temperatures: Reassessment of the Rate of Cooling by the CO₂ 15- μ m Emission in the Lower Thermosphere, *Izvestiya Atmos. Ocean. Phys.*, 38, 613–624, 2002.
- Kumer, J. B. and James, T. C.: SPIRE data evaluation and nuclear IR fluorescence processes, Report DNAOOI-79-C-0033, AFGL, Bedford, Mass., 1983.
- Kutepov, A. A., Gusev, O. A., and Ogibalov, V. P., Solution of the non-LTE problem for molecular gas in planetary atmospheres: Superiority of accelerated lambda iteration, *J. Quant. Spectrosc. Radiat. Transf.* 60, 199, 1998.
- Kutepov, A. A., Feofilov, A. G., Marshall, B. T., Gordley, L. L., Pesnell, W. D., Goldberg, R. A., and Russell III, J. M.: SABER temperature observations in the summer polar mesosphere and lower thermosphere: Importance of accounting for the CO₂ ν_2 quanta V–V exchange, *Geophys. Res. Lett.*, 33, L21809, doi:10.1029/2006GL026591, 2006.
- Lara-Castells, de, M. P., Hernández, M. I., Delgado-Barrio, G., Villarreal, P., and López-Puertas, M.: Vibrational quenching of CO₂(010) by collisions with O(³P) at thermal energies: a quantum-mechanical study, *J. Chem. Phys.*, 124, 164302, doi:10.1063/1.2189860, 2006.
- Lilenfeld, H. V.: Deactivation of Vibrationally-Excited NO and CO₂ by O-Atoms, Final technical rept., 28 September 89–15 June 94, <http://handle.dtic.mil/100.2/ADA298581> (last access: September 2012), ADA298581, 1994.
- López-Puertas, M. and Taylor, F. W.: Non-LTE Radiative Transfer in the Atmosphere, Singapore: World Scientific, 2001.
- López-Puertas, M., López-Valverde, M. A., Rinsland, C. P., and Gunson, M. R.: Analysis of the Upper Atmosphere CO₂(ν_2) Vibrational Temperatures Retrieved From ATMOS/Spacelab 3 Observations, *J. Geophys. Res.*, 97, 20469–20478, 1992.
- Mlynczak, M. G. Hunt, L. H., Mast, J. C., Marshall, B. T., Russell III, J. M., Smith, A. K., Siskind, D. E., Yee, J.-H., Mertens, C. J., Martin-Torres, F. J., Thompson, R. E., and Gordley, L. L.: Atomic Oxygen in the Mesosphere and Lower Thermosphere Derived from SABER, *J. Geophys. Res.*, submitted, 2012.
- Offermann, D., Grossmann, K. U., Barthol, P., Knieling, P., Riese, M., and Trant, R.: Cryogenic Infrared Spectrometers and Telescopes for the Atmosphere (CRISTA) experiment and middle atmosphere variability, *J. Geophys. Res.*, 104, 16311–16325, doi:10.1029/1998JD100047, 1999.
- Ogibalov, V. P.: The CO₂ Non-LTE Problem Taking Account of the Multiquantum Transitions on the ν_2 -Mode During CO₂-O Collisions, *Phys. Chem. Earth (B)*, 25, 493–499, 2000.
- Pollock, D. S., Scott, G. B. I., and Phillips, L. F.: Rate constant for quenching of CO₂(010) by atomic oxygen, *Geophys. Res. Lett.*, 20, 727–729, 1993.
- Ratkowski, A. J., Picard, R. H., Winick, J. R., Grossmann, K. U., Homann, D., Ulwick, T. J. C., and Paboojian, A. J.: Lower-thermospheric infra-red emissions from minor species during high-latitude twilight–B. Analysis of 15 μ m emission and comparison with non-LTE models, *J. Atmos. Terr. Phys.*, 56, 1899–1914, 1994.
- Remsberg, E. E., Marshall, B. T., Garcia-Comas, M., Krueger, D., Lingenfelter, G. S., Martin-Torres, J., Mlynczak, M. G., Russell III, J. M., Smith, A. K., Zhao, Y., Brown, C., Gordley, L. L., Lopez-Gonzalez, M. J., Lopez-Puertas, M., She, C.-Y., Taylor, M. J., and Thompson, R. E.: Assessment of the quality of the Version 1.07 temperature-versus-pressure profiles of the middle atmosphere from TIMED/SABER, *J. Geophys. Res.*, 113, 1–27, doi:10.1029/2008JD010013, 2008.
- Rezac, L.: Simultaneous retrieval of $T(p)$ and CO₂ volume mixing ratio from limb observations of infrared radiance under non-LTE conditions, Ph.D. thesis, <http://dl.dropbox.com/u/44230060/Ladislav-Rezac-PhD-thesis-2011.pdf>, Hampton University of Virginia, 163 pp., 2011.
- Russell III, J. M., Mlynczak, M. G., Gordley, L. L., Tansock, J. J., and Esplin, R.: Overview of the SABER experiment and preliminary calibration results, *Proc. SPIE, Opt. Spectr. Tech. and Instrum. for Atm. and Space Res. III*, 3756, 277–288, 1999.
- Sharma, R. D.: Infrared airglow, *Progress in Atmospheric Physics: Proceedings of the 15th Annual Meeting on Atmospheric Studies by Optical Methods*, edited by: Rodrigo, R., López-Moreno, J. J., López-Puertas, M., and Molina, A., Kluwer Academic Publishers, Boston, 177–186, 1987.
- Sharma, R. D. and Nadile, R. M.: Carbon dioxide (ν_2) radiative results using a new non-equilibrium model, AIAA-81-0426, AIAA 19th Aerospace Sciences Meeting St. Louis, 1981.
- Sharma, R. D. and Wintersteiner, P. P.: Role of carbon dioxide in cooling planetary thermospheres, *Geophys. Res. Lett.*, 17, 2201–2204, 1990.
- Sharma, R., Zygelman, B., von Esse, F., and Dalgarno, A.: On the relationship between the population of the fine structure levels of the ground electronic state of atomic oxygen and the translational temperature, *Geophys. Res. Lett.*, 21, 1731–1734, 1994.
- She, C.-Y., Sherman, Y. J., Yuan, T., Williams, B. P., Arnold, K., Kawahara, T. D., Li, T., Xu, L. F., Vance, J. D., Acott, P., and Krueger, D. A.: The first 80-hour continuous lidar campaign for simultaneous observation of mesopause region temperature and wind, *Geophys. Res. Lett.*, 30, 1319–1323, doi:10.1029/2002GL016412, 2003.
- Sheese, P. E., McDade, I. C., Gattinger, R. L., and Llewellyn, E. J.: Atomic oxygen densities retrieved from Optical Spectrograph and Infrared Imaging System observations of O₂ A-band airglow emission in the mesosphere and lower thermosphere, *J. Geophys. Res.*, 116, D01303, doi:10.1029/2010JD014640, 2011.
- Shizgal, B.: Energy distribution function of translationally hot O(³P) atoms in the atmosphere of Earth, *Planet. Space Sci.*, 27, 1321–1332, 1979.

- Shved, G. M., Khorostovskaya, L. E., Yu. Potekhin, I., Demyanikov, A. I., Kutepov, A. A., and Fomichev, V. I.: Measurement of the quenching rate constant for collisions CO₂ (01¹0)-O: The importance of the rate constant magnitude for the thermal regime and radiation of the lower thermosphere, *Izvest. Atmos. Oceanic. Phys.*, 27, 431–437, 1991.
- Shved, G. M., Kutepov, A. A., and Ogibalov, V. P.: Non-local thermodynamic equilibrium in CO₂ in the middle atmosphere. I. Input data and populations of the ν_3 mode manifold states, *J. Atmos. Sol. Terr. Phys.* 60, 289–314, 1998.
- Smith, M. D., Pearl, J. C., Conrath, B. J., and Christensen, P. R.: Thermal Emission Spectrometer results: Mars atmospheric thermal structure and aerosol distribution, *J. Geophys. Res.*, 106, 23929–23945, 2001.
- Smith, A. K., Marsh, D. R., Mlynczak, M. G., and Mast, J. C.: Temporal variations of atomic oxygen in the upper mesosphere from SABER, *J. Geophys. Res.*, 115, D18309, doi:10.1029/2009JD013434, 2010.
- Smith, A. K., Garcia, R. R., Marsh, D. R., and Richter, J. H.: WACCM simulations of the mean circulation and trace species transport in the winter mesosphere, *J. Geophys. Res.*, 116, D20115, doi:10.1029/2011JD016083, 2011.
- Stair Jr., A. T., Sharma, R. D., Nadile, R. M., Baker, D. J., and Grieder, W. F.: Observations of Limb Radiance With Cryogenic Spectral Infrared Rocket Experiment, *J. Geophys. Res.*, 90, 9763–9775, 1985.
- Taylor, R.: Energy Transfer Processes in the Stratosphere, *Can. J. Chem.*, 52, 1436–1451, 1974.
- Vollmann, K. and Grossmann, K., U.: Excitation of 4.3 μm CO₂ emissions by O(¹D) during twilight, *Adv. Space. Res.*, 20, 1185–1189, 1997.
- Xu, J., Gao, H., Smith, A. K., and Zhu, Y.: Using TIMED/SABER nightglow observations to investigate hydroxyl emission mechanisms in the mesopause region, *J. Geophys. Res.*, 117, D02301, doi:10.1029/2011JD016342, 2012.